



Quantifying the extent of crushing in granular materials: A probability-based predictive method

G. Marketos^{*}, M.D. Bolton

Soil Mechanics Group, Engineering Department, University of Cambridge, UK

Received 16 November 2006; accepted 12 March 2007

Abstract

Grain crushing is one of the micromechanisms that governs the stress–strain behaviour of a granular material, and also its permeability by altering the grain size distribution. It is therefore advantageous to be able to predict the point of onset of crushing and to quantify the subsequent evolution of crushing. This paper uses the data of Discrete Element Method (DEM) simulations to inform a statistical model of granular crushing. Distributions of normalised contact forces are first obtained. If the statistical distribution of the crushing strength of the grains is then known, the onset of crushing within an assembly of grains should be predictable. Two different cases, one in which grain strength was statistically independent of grain size and one showing an arbitrary trend, were used to compare with DEM results and so confirm the validity of the statistical method.

© 2007 Elsevier Ltd. All rights reserved.

Keywords: Particle crushing; Granular material; Probability and statistics; Discrete Element Method; Force distribution

1. Introduction

Sand grain crushing, through its effect on grain size distribution, has long been identified as one of the micromechanisms governing the stress–strain behaviour of sand. More recently McDowell and Bolton (1998) have related the normal compression line of sand to fractal crushing of particles, while Cheng et al. (2004) have shown that the yield surface of a sand can be interpreted as a contour of crushing. Furthermore, constitutive models that

^{*}Corresponding author. Tel. +44 1223742371; fax: +44 1223460777.

E-mail address: gm256@cam.ac.uk (G. Marketos).

attempt to include the constantly changing grain size distribution as a stress-related parameter have started taking shape (Einav, 2007; Muir Wood, 2006).

In addition, particle crushing reduces the mean particle size of a sample, consequently reducing its mean pore size, something that directly affects its permeability. Crushing is usually homogeneously distributed in a sample, but there are questions whether it might localise into thin tabular zones similar to the ‘compaction bands’ observed by Baud et al. (2004) in bonded granular rocks. Grain crushing could also be directly related to sanding in oil wells, as the fines produced can be transported through the larger pores into the oil well, or might block a pore completely.

Experimental tests of grain crushing within sand samples are not easy to interpret since the evolution of grain damage will not be obvious even after a careful post-test inspection. There is therefore a need for a theoretical model of the onset and evolution of crushing extent inside a granular assembly, so that the best use can be made of post-test observations, and so that grain crushing strength can be included explicitly in continuum constitutive models.

Nakata et al. (1999) described experiments to relate the extent of crushing in an assembly of grains under stress to the crushing strength of individual particles. In these experiments a small number of particles were pre-selected and photographed so that damage to them could be tracked by exhumation and photography after stressing. As the force distribution inside the sample was not known, the simplifying assumption of equal force causing crushing of all particles was adopted. This may lead to inaccurate deductions, as the force distribution has been seen to be far from uniform, following an exponential tail decay for large forces (Thornton, 1997; Radjai et al., 1996).

To overcome these difficulties three-dimensional Discrete Element Method (DEM) computer simulations of a sand specimen have been conducted. This allows easy access to the multitude of data involved yielding information on micromechanical parameters of interest (such as the internal grain-force distribution) which would otherwise be inaccessible. Data presented here were obtained by two different sets of computer simulations. The first set was performed in model sand with unbreakable particles so as to obtain the evolution of the distribution of inter-particle forces. Another set of simulations was performed on sand with crushable particles, to obtain the evolution of crushing. The results of our proposed statistical analysis will be then compared with the crushing simulation results to confirm the validity of the new statistical model. Insight gained here will allow, among others, the development of further statistical tools that are needed to understand and describe the possible localisation of crushing inside a sample.

2. The discrete element method

The simulations outlined here were performed using the commercially available software code PFC^{3D} developed by Itasca Consulting Group Inc. (2003) and based on the work of Cundall and Strack (1979). This is a three-dimensional Discrete Element Code, where the individual grains are represented as spheres. A concise description can be found in the PFC^{3D} manual (Itasca Consulting Group Inc., 2003). The sample used for all simulations consists of 8943 particles with radii uniformly distributed between 1 and 2 mm. The assembly is cuboidal in shape, with an initial porosity of 44.8% at zero applied stress and initial dimensions of 60 mm × 60 mm × 72 mm. It was prepared by numerically simulating ‘dry pluviation’ inside rigid, frictionless plane walls. One should note that all simulations

reported here were performed on unbonded particles. In one set of simulations a model of crushing was implemented. This involved removing particles when a limiting normal contact force was reached, the value of which was either independent, or a function of, particle size. Removal is thought to represent crushing in the case when a brittle grain is reduced to dust-like fragments. A similar crushing model was implemented by Couroyer et al. (2000).

In all simulations reported here the side walls were kept fixed in position while the top and bottom walls were both moved inwards so as to simulate one-dimensional compression with a shortening rate of 100 mm/s. In performing the simulations only the particles that were lying beyond 3 mean particle diameters (i.e. 9 mm) away from the top and bottom boundaries were allowed to crush. This was done so as to avoid any artificial crushing localisations due to the smaller particle density and the non-random grain structure produced by the boundary. Only the internal region was interrogated for contact forces during the subsequent simulations. No gravity forces were included, and a soft contact approach was used. The micromechanical parameters used in the simulations can be found in Table 1. The values of these parameters were chosen to be of the order of magnitude inferred from single crushing tests on quartz particles reported by Nakata et al. (1999).

2.1. Simulations with no crushing: the contact force probability density function (pdf)

The first set of simulations was performed on the sample with non-crushable particles. The aim of this was to obtain the evolution of probability density of the normal contact force with increasing mean force in a granular assembly. The normal contact force distribution was monitored as the stress in the sample was increased in the one-dimensional compression test. When the normal force was non-dimensionalised by its mean value the distributions for different stress levels were seen to collapse on the same curve (plotted on linear and semi-logarithmic axes in Fig. 1a and b, respectively). One should note that a pdf has been plotted here. Consequently the probability of finding a normalised force with magnitude between x and $x + \Delta x$ will be given by the area under the curve of Fig. 1a. It was found that this curve has an exponential tail for large forces, as reported in the literature (e.g. Radjai et al., 1996 or Thornton, 1997). A functional fit to the mean curve, of the form $(x + \Delta)^B \cdot e^{-\Gamma x + E}$, where B , Γ , Δ , and E are constants, has also been included in the diagram.

Table 1
Micromechanical parameters used for the simulation

Parameter	Numerical value
Normal and shear stiffness of balls	4×10^6 N/m
Normal and shear stiffness of walls	4×10^6 N/m
Particle friction coefficient, μ_b	0.5
Wall friction coefficient, μ_w	0.0
Density of spheres	2650 kg/m ³
Coefficient of local damping	0.7
Sample shortening rate	100 mm/s

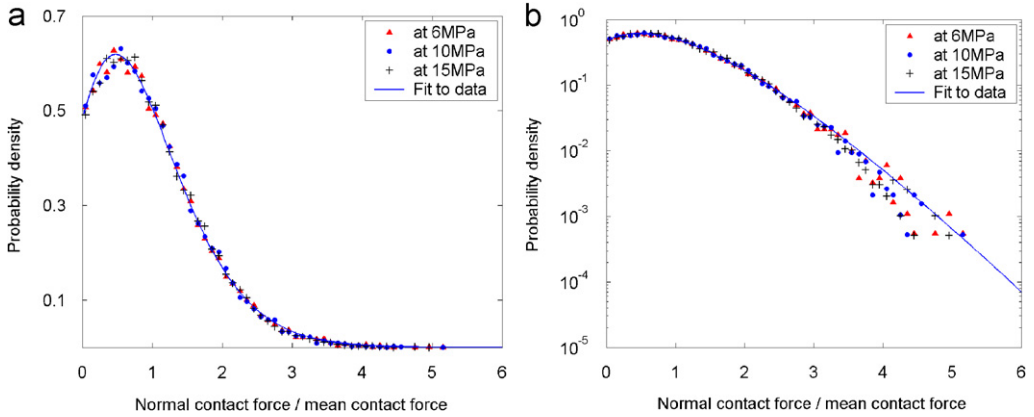


Fig. 1. A plot of the probability density function of normal contact force over mean contact force for three different stress levels. Plotted on (a) linear and (b) semi-logarithmic axes.

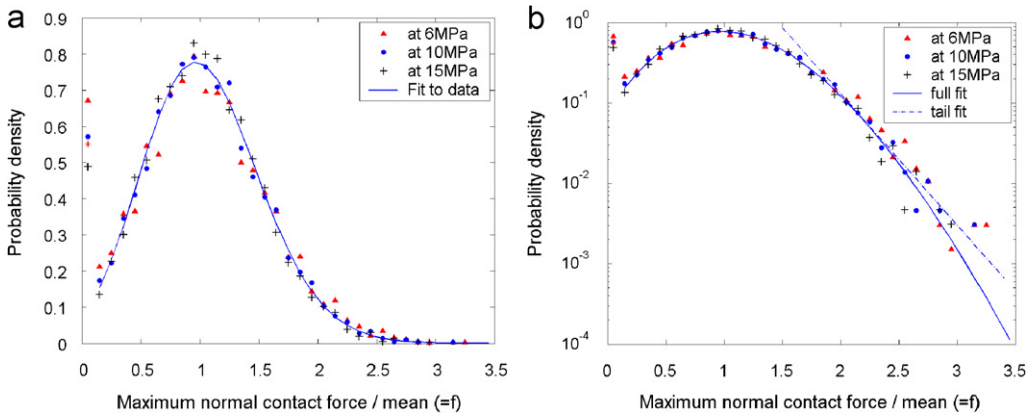


Fig. 2. A plot of the probability density function of maximum normal contact force for a particle over mean maximum normal contact force for three different stress levels. Plotted on (a) linear and (b) semi-logarithmic axes.

This pdf characterises the state of each contact. However, as each particle will have a variable number of contacts with other particles around it, this pdf cannot lead to the prediction of crushing unless the distribution of the coordination number of particle contacts is known. Furthermore the way in which the probability of crushing is calculated will depend on the exact breakage criterion used. Criteria commonly used in the literature have ignored the effect of coordination number on the breakage of particles, and in the majority of cases a criterion based on a threshold of force or pressure on a particle has been implemented (e.g. Åström and Herrmann, 1998; Couroyer et al., 2000). This method will be also followed here.

In this case the distribution of the maximum contact force acting on a particle, and not the distribution of all contact forces, is relevant. This has been plotted in Fig. 2, again for the same three stress levels. The plots of probability density versus non-dimensionalised force again seem to collapse to the same curve. The mean curve for a range of stress levels

was fitted with a function of the form

$$g(f) = (f + a)^b e^{-cf-d} \quad \text{with } a = 2.6, b = 53, c = 15, d = 54, \quad (1)$$

where f is the ratio of the maximum normal contact force on a given particle to its mean value for all particles. As before, the force pdf has been plotted on both linear and semi-logarithmic axes in Fig. 2a and b. As seen in Fig. 2b, for forces larger than $2 F_{\text{mean}}$ the distribution can be approximated by an exponential decay of the form

$$g(f) = \alpha e^{-\beta f} \quad \text{with } \alpha = 247, \beta = 3.77. \quad (2)$$

This exponential fit has also been included in the figure.

2.2. Simulations with crushing

A second set of simulations was performed, this time with the introduction of a model of grain crushing. At each timestep during the simulation the normal force at each contact was monitored and a particle was removed whenever this force exceeded a certain threshold. Two different crushing simulations were conducted; one where the limiting force was randomly assigned to a particle and another where the limiting force was linked to particle size through a limiting characteristic stress. These two different simulations were performed so as to allow the statistical method proposed here to be developed and validated for two completely different physical cases.

The first simulation models the case where the distribution of the strength parameter is strongly dependent on the existence of internal flaws in the particles, with randomness overriding any size-effect. The second simulation ignores completely the effect of the internal flaws and focuses on the effect of the size of a particle, as it is assumed that in this case there is a limiting value of a stress-like parameter that will govern failure of a particle. Of course in reality both these effects come into play, and it will be shown that the statistical model which emerges can incorporate this more complicated case also. Finally one should note that no attempt has been made to model the effect of the coordination number on the breakage of particles. This is known to have an effect on particle breakage (e.g. Tsoungui et al., 1999). However in situations where the grain size distribution is not wide, the standard deviation of coordination numbers around the mean will be small. This is the case relevant to this study, and so, the effect of a varying coordination number for particles has been ignored.

2.3. Simulation where strength is independent of particle size

As mentioned above, the limiting force at which a particle would break was chosen from a certain distribution, independently of particle size. This distribution was chosen arbitrarily to be of the form

$$h(\Phi) = 0.0395/\sqrt{\Phi} \quad (3)$$

lying between the limits $\Phi_{\text{max}} = 640 \text{ N}$ and $\Phi_{\text{min}} = 160 \text{ N}$ where Φ is the characteristic strength parameter in Newtons. Numbers distributed according to Eq. (3) are randomly assigned to grains. One should note that this work only describes the development of a statistical method to predict crushing, and any distribution would be sufficient. Other possible choices for the strength distribution might include a uniform variation, a normal

or most probably a Weibull distribution of particle strength as proposed by a number of researchers (e.g. McDowell and Amon, 2000; Nakata et al., 1999), and would be highly dependent on the grain material and the depositional environment or stress-history of the granular assembly. The actual inputs to the simulation that lie approximately on the curve of Eq. (3) are plotted in Fig. 3.

The stress–strain curve for this simulation is plotted in Fig. 4. The crush rate versus strain has also been included in this figure. The initial response up to 0.05 strain is only due to particle rearrangement with slipping at contacts initiated by elastic shortening at the contacts. Crushing of particles is initiated at a strain of 0.053. As more particles crush the

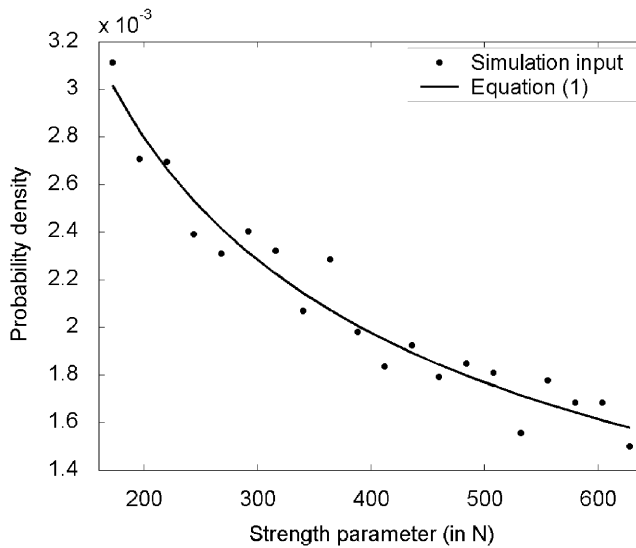


Fig. 3. A plot of the distribution of strength parameters as used in the simulation and as approximated by Eq. (3).

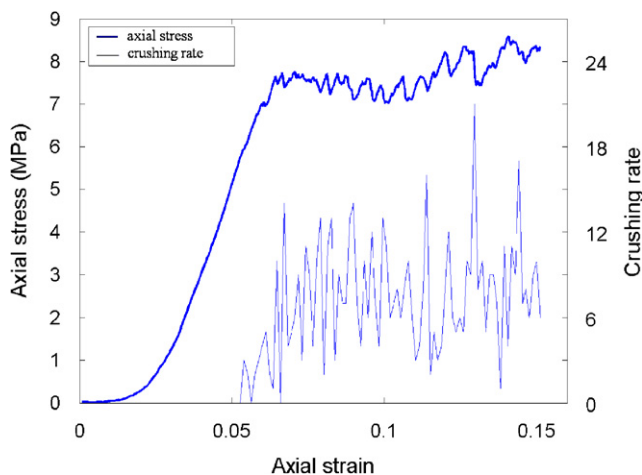


Fig. 4. The axial stress and crushing rate (similar to acoustic emission data) plotted versus strain for the case where grain strength is independent of grain size.

stiffness of the sample decreases and a crushing plateau is reached beyond a strain of 0.065. One should note that the stress–strain curve exhibits instabilities, which for similar simulations have been shown to correspond to localised crushing (Marketos and Bolton, 2005). Various other micromechanical parameters were traced throughout this simulation and were used to check the validity of the proposed statistical analysis outlined below.

2.4. Simulation where strength is a function of particle size

A limit on the characteristic stress of each particle, defined as the maximum normal contact force divided by the square of the diameter, was implemented here. This normalisation represents the limiting stress state inside a grain. Even though the exact configuration of forces in three dimensions is disregarded it is clear from dimensional considerations that this characteristic stress must be proportional to the maximum tensile stress developed inside a grain: McDowell and Amon (2000), Nakata et al. (1999). In this case its value was chosen to be uniform for each particle, at 40 MPa. It should be noted that a statistical distribution of the limiting characteristic stress parameter could be implemented equally. For brevity this will not be expanded. The curves of stress and crush rate versus strain for this simulation are plotted in Fig. 5. All features observed in Fig. 4 can also be seen here.

2.5. Statistical Analysis: strength independent of grain size

The probability of two statistically independent events both occurring is given by the product of the two individual probabilities. In the case discussed here the crushing criterion is implemented as a limiting normal contact force, and so the probability of crushing for a particle will be just the probability that the maximum normal contact force on it exceeds its strength. One can identify event 1 as the particle having a given strength and event 2 as the force on the particle exceeding this strength value. Further assuming that these two events are independent, which may initially seem an acceptable assumption,

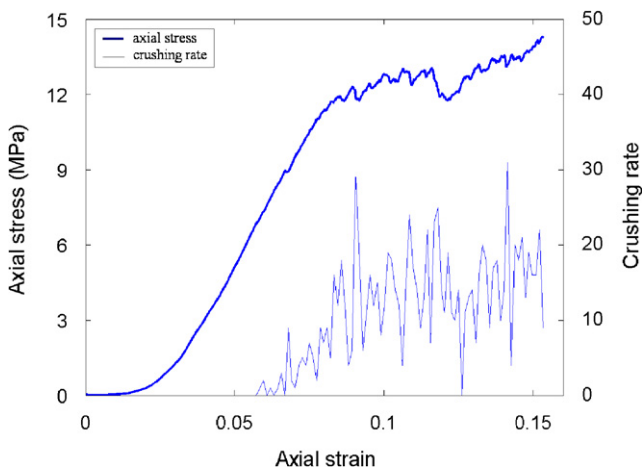


Fig. 5. The axial stress and crushing rate (similar to acoustic emission data) plotted versus strain for the case where grain strength is a function of grain size.

one can write the probability of crushing of a given particle with strength ϕ as the integral of Eq. (4) below.

$$p = \int_{\phi}^{+\infty} g(f) \, df. \quad (4)$$

Here p is the probability of crushing of a specific particle at a given macroscopic stress, ϕ and f are this particle's strength and maximum particle force, respectively, each non-dimensionalised by the mean of the maximum force on all particles, and g is the pdf for maximum particle normal force as plotted in Fig. 2 and given by Eq. (1) or (2).

Eq. (4) will indeed be the probability of crushing inside a granular sample made up of a collection of particles having the same strength, Φ (or ϕ if non-dimensionalised by the mean maximum particle force). This, however, is very rarely the case. The analysis can be extended to the case where the strength of the particles itself follows a certain distribution. Now there is also a probability associated with the strength of the particle having a certain value (as plotted for this study in Fig. 3). The probability of a crushing event will then be given by the summation of the products of the probabilities of the two independent events: the probability that the strength has a value Φ , and that the grain-force is larger than Φ . This should be done for all possible values of particle strength. In the limit of continuous distributions for both the above quantities the summation becomes an integral and the probability of a crushing event is given by Eq. (5). This is sometimes termed the convolution integral.

$$P = \int_{\text{Strength}_{\min}}^{\text{Strength}_{\max}} p(\text{Strength} = \Phi) p(\text{Force} > \Phi) \, d\Phi. \quad (5)$$

The next step involves a change of variable inside the integral calculating the probability of force exceeding Φ , as g , the force pdf, is in terms of normalized force (f), while Φ is a force in Newtons. This is how the mean force term (\bar{F}) comes into the calculation, and the result is given in Eq. (6) below.

$$P = \int_{\Phi_{\min}}^{\Phi_{\max}} h(\Phi) \left(\int_{\Phi}^{+\infty} g(F/\bar{F}) \, dF/\bar{F} \right) d\Phi \quad (6)$$

$$= \int_{160}^{640} \frac{0.0395}{\sqrt{\Phi}} \left(\int_{\Phi}^{+\infty} (F/\bar{F} + 2.6)^{53} e^{-15F/\bar{F} - 54} \, dF/\bar{F} \right) d\Phi. \quad (7)$$

Substituting the relevant probability distribution functions into Eq. (6) gives Eq. (7) above. This integral equation can easily be implemented numerically to give the probability of crushing and this has been plotted in Fig. 6. One should note that as the mean force term is a direct measure of the stress state in each particular stress path, there is an implication of a relation between the extent of crushing (and therefore grain size distribution in a real sand sample) and stress.

As only the large forces inside a sample will be the ones that will cause crushing, one can use the approximation of the exponential tail to describe the force distribution. This allows for a significant simplification to the calculation. In our case, substituting the approximation to the force pdf given in Eq. (2) into Eq. (6) gives Eq. (8). The integral of Eq. (8) can now be performed analytically, and this will be the case for other

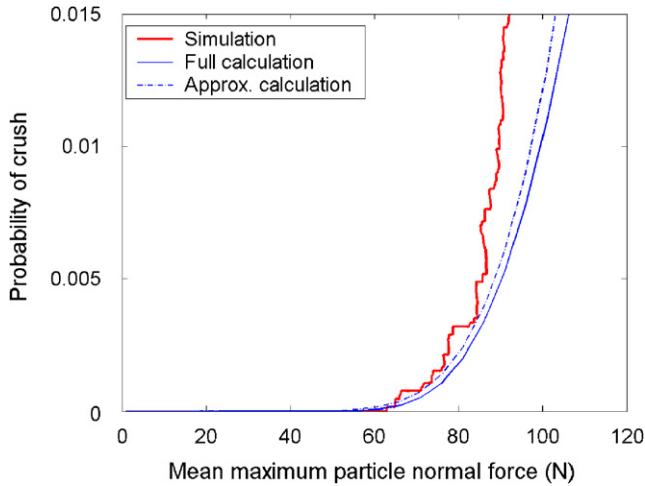


Fig. 6. A plot of the probability of one crush versus mean maximum particle force as given by Eqs. (7) (using the full force pdf) and (8) (using the exponential tail approximation). Note that these correspond to the smooth curves in this plot. The results of the crushing simulations are also plotted for comparison.

grain-strength distributions.

$$P = \int_{160}^{640} \frac{0.0395}{\sqrt{\Phi}} \left(\frac{1}{\bar{F}} \int_{\Phi}^{+\infty} 247e^{-3.77F/\bar{F}} dF \right) d\Phi. \quad (8)$$

The result for the probability of a crush obtained using the exponential tail approximation has also been plotted in Fig. 6 for comparison. One should note that there is no significant difference between these two curves, demonstrating that the use of the exponential tail is sufficient.

A plot of the results of the crushing simulations for the case where strength is independent of particle size has been included in Fig. 6. This probability was calculated as the ratio of the cumulative count of particles that have crushed at each instant over the total number of particles in the simulation initially. One observes that the crushing calculation and the simulation results agree very well initially and up to a mean maximum particle normal contact force of 80 N. Furthermore, the calculations can predict very well when the first crushing will occur. However the curves diverge from each other at higher mean forces as the crushing events stop being independent of each other.

2.6. Strength is a function of grain size

The case relevant to the second set of crushing simulations, where the crushing strength is a function of particle diameter, will now be considered. As mentioned above, a different crushing criterion has been implemented in these simulations. Here a limit in the characteristic stress inside each particle (calculated as the maximum normal contact force divided by the square of the particle diameter following McDowell and Amon, 2000 or Nakata et al., 1999) has been enforced. This limit has been set to be constant at 40 MPa for every particle, for simplicity. This implies that smaller particles will crush more easily as a smaller force will be enough to produce the same characteristic stress as in a larger particle.

Keeping in mind that the grain diameter is uniformly distributed between 2 mm (D_{\min}) and 4 mm (D_{\max}), one can obtain the distribution of strength for particles based on normal contact force, as before. Starting from an equation which describes the integral of the pdf of grain size and with a single change of variable (as $\sigma = \Phi/D^2$) we obtain Eq. (9). This is the integral of a distribution of strength based on limiting force identical to the one of Eq. (3).

$$\int_{D_{\min}}^{D_{\max}} p(\text{Diameter} = D) dD = \int_{D_{\min}}^{D_{\max}} \frac{1}{D_{\max} - D_{\min}} dD = \int_{\Phi_{\min}}^{\Phi_{\max}} \frac{1}{(D_{\max} - D_{\min})} \times \frac{1}{2\sqrt{\sigma\Phi}} d\Phi = \int_{160}^{640} \frac{0.0395}{\sqrt{\Phi}} d\Phi. \quad (9)$$

This is the justification for the initial selection of this particular distribution. At first one might think that if the two strength distributions are the same, the crushing probabilities at the same mean force must also be the same. This proved not to be the case, as can be inferred from the different stress levels at which the two simulations reached the crushing plateau (see Figs. 4 and 5). This demonstrates that the assumption of force and particle-strength independence is no longer valid. One should therefore re-examine the force distribution in order to identify any dependence on particle size.

Separating the randomly positioned particles into subsets according to their radius, the mean maximum normal contact force in each subset (as non-dimensionalised by mean maximum normal contact force for all particles) is plotted versus particle size in Fig. 7. The relationship is identical for three different stress levels, and it can be seen that the mean force varies approximately linearly with particle radius. A similar linear relation has been reported by Török et al. (2005) for a large number of different simulations under different conditions. One might therefore draw the conclusion that this linear relation is a universal phenomenon.

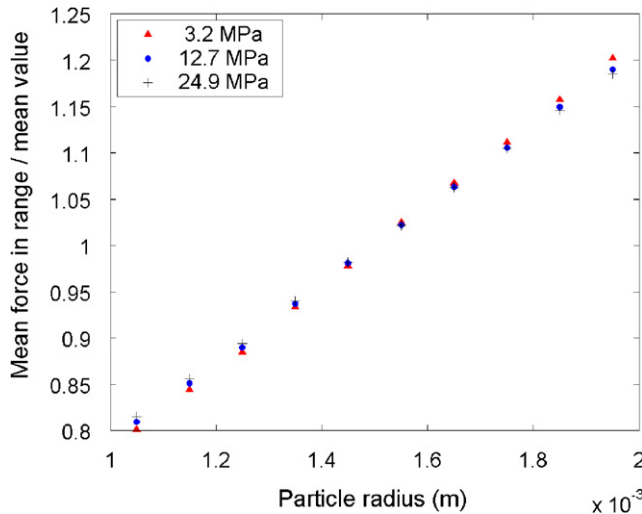


Fig. 7. A plot of the mean of the maximum normal contact force in each particle size range (as non-dimensionalised by the mean value for all particles) versus particle radius for three different stress levels.

It therefore becomes clear that particle-size dependence of contact forces should be included in the statistical analysis of the extent of crushing for the case where particle strength is a function of radius. The average maximum particle force carried by a grain increases linearly with grain radius. In this second simulation, however, the resistance to crushing is proportional to the square of the particle radius, meaning that the forces on larger particles will now be unlikely to break these stronger particles, leading to the crushing plateau being observed at larger stresses as seen in Fig. 5 compared with Fig. 4. From Fig. 7 particles with a radius of 2 mm will carry on average a force which is 1.2 times the mean maximum particle force, whereas the 1 mm particles will carry an average force of 0.8 times the mean. This translates to a characteristic particle stress proportional to $1.2/2^2 = 0.3$ for the larger particles and $0.8/1^2 = 0.8$ for the smaller. This means that smallest particles compared with the largest will on average be carrying a larger characteristic stress by a factor of 2.7. This leads to their preferential crushing when a constant characteristic strength of particles is implemented. For comparison, in the simulations where the resistance to crushing was independent of particle size, the larger particles would preferentially crush, as these carried larger forces. A modification to the statistical prediction is therefore necessary, requiring the calculation of the pdf of maximum particle force as a function of particle size.

Data from the simulations without crushing were used to produce Fig. 8. Again the particles were divided into ranges, according to their size. In each size range the pdf for particle maximum normal contact force was calculated from the data. This was followed throughout the no-crushing simulation, and was found to be relatively invariant with stress level. A plot of the mean pdf of force for each radius range has been plotted in Fig. 8a. One should note that the force axis has been non-dimensionalised by the mean maximum particle normal force, while the radius axis is again in non-dimensional form. The radius index I_R , which will range from 0 to 1 for any grain size distribution, is given by

$$I_R = (R - R_{\text{minimum}})/(R_{\text{maximum}} - R_{\text{minimum}}). \quad (10)$$

A fit for this two-dimensional function was attempted and this has been plotted in Fig. 8b. The form of this function is relatively complicated but a very good fit is given by Eq. (11). The fitting function was made up of two functions, one that resembles a normal distribution, and one that is an exponential decay, according to the value of the variable

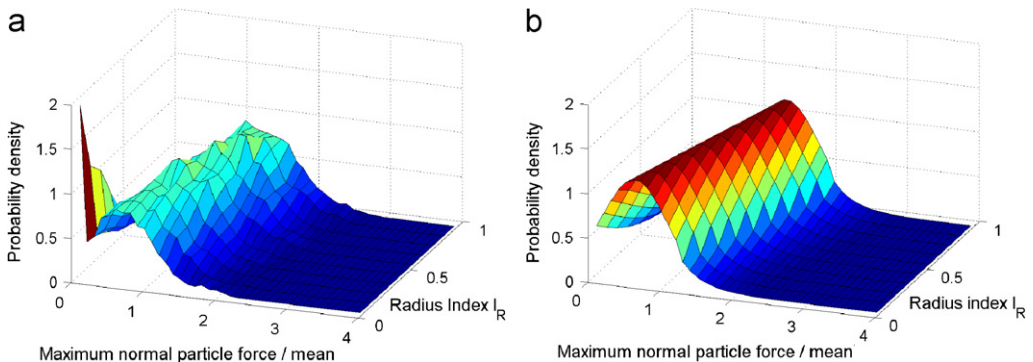


Fig. 8. The data (Fig. 8a) and the fit (Fig. 8b) of the probability density function for maximum normal particle force in each size range.

$(f \cos \theta + I_R \sin \theta)$.

$$G(f, I_R) = \frac{A_1}{\sigma\sqrt{2\pi}} e^{-(f \cos \theta + I_R \sin \theta - \mu)^2 / 2\sigma^2} \quad \text{for } f \cos \theta + I_R \sin \theta \leq 0.9$$

$$G(f, I_R) = A_2 e^{B_2(f \cos \theta + I_R \sin \theta)} \quad \text{for } f \cos \theta + I_R \sin \theta > 0.9$$

with $A_1 = 0.74, \mu = 0.40, \sigma = 0.34, A_2 = 20.3, B_2 = -4.67, \theta = -41.6^\circ$. (11)

Note again that the statistical analysis only requires a plausible function as an input for the two-dimensional pdf, which can be supported by the user’s data. Any function can easily be implemented as all the numerical integrations can be performed by a standard computer package. The way to incorporate this pdf into the statistical analysis will now be presented.

2.7. Statistical analysis for the case where the strength is a function of radius

The same statistical principles apply to this case also. As the strength will now be a function of particle size the probability of a particle of radius index I_R crushing will be given by the convolution integral of Eq. (12).

$$P = \int_{\text{Strength}_{\min}}^{\text{Strength}_{\max}} p(\text{Strength} = \Phi, I_R) p(\text{Force} > \Phi, I_R) d\Phi. \quad (12)$$

As there is a pdf that describes the grain size distribution, denoted by $k(I_R)$ (a function of radius index), the probability of crushing for all particles will require the calculation of a further convolution. This is shown in

$$P = \int_{I_{\min}}^{I_{\max}} \left\{ \int_{\text{Strength}_{\min}}^{\text{Strength}_{\max}} p(\text{Strength} = \Phi, I_R) p(\text{Force} > \Phi, I_R) d\Phi \right\} k(I_R) dI_R. \quad (13)$$

This is the full equation for the case where we have a distribution of strengths for each different particle size range. In our case, however, the value of I_R will define a specific value of force that causes crushing, which is equal to

$$\Phi_{\text{crush}} = 4\sigma_{\text{crush}} [I_R (R_{\max} - R_{\min}) + R_{\min}]^2. \quad (14)$$

The inner integral of Eq. (13) will then become

$$P = \int_{I_{\min}}^{I_{\max}} p(\text{Force} > \Phi_{\text{crush}}, I_R) k(I_R) dI_R. \quad (15)$$

In this case the size distribution is uniform, and so there will be the same probability associated with every I_R . Furthermore, care has to be taken when substituting Eq. (11) into Eq. (15), as the former is in terms of non-dimensionalised force, while the latter is not. Eq. (15) was implemented numerically in the Matlab software package and the results for the probability of one crush versus mean maximum particle normal contact force are plotted in Fig. 9. The probability of one crush as calculated from the second crushing simulation is also included for comparison. This was obtained as the ratio of the cumulative count of particles that have crushed at each instant over the total number of particles initially in the active region of the simulation.

One can observe in this graph that the statistical analysis has succeeded in predicting the mean force at which the first crush will happen. Furthermore, the observed and calculated curves agree with each other over the initial mean force range and up to 120 N.

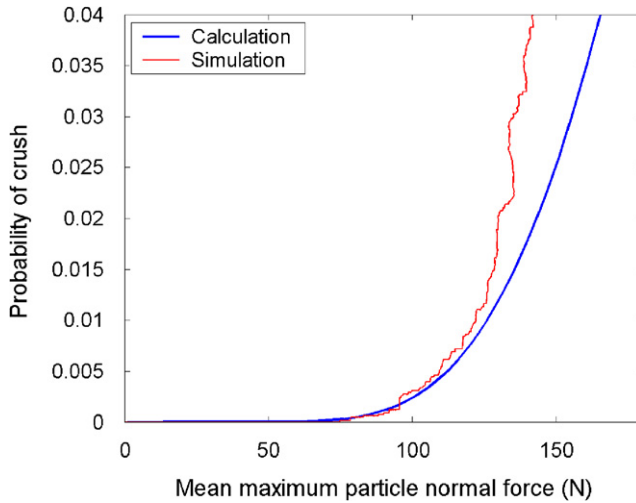


Fig. 9. A plot of the probability of one crush versus mean maximum particle force as given by Eq. (15), for the case where grain strength is a function of grain size.

The curves then diverge, as the crushing events stop being independent of each other, as already seen in Fig. 6.

3. Conclusions

This article presents a new approach to treating granular materials, describing variability using statistics and then combining the statistical descriptors with probabilistic arguments to quantify and predict the evolution of a micromechanics parameter. This has rarely been attempted in granular materials, and may serve as an example of how probability and statistics can be applied to assemblies of brittle grains. As current research in granular materials moves away from empirical continuum mechanics to identify relevant micromechanisms, so that microparameters can be linked to continuum mechanics parameters, the statistics of grain properties becomes increasingly important. Recent advances in technology (especially computing power and DEM) make micromechanics data more readily available to engineers. Therefore approaches similar to the one reported here should soon become available in practical applications.

A statistical method for quantifying the extent of crushing has been proposed and tested against crushing simulations. The assumption underlying this method is that of statistical independence of crushing events. As long as this simple assumption holds, the method has been shown to give very good results. Approaches based on this method can be used to identify the mean force (and hence the stress level) at which first breakage of particles is to be expected. This might be important in cases where particles that are products of a well-controlled manufacturing process are stressed (e.g. in transportation or storage), and minimisation of breakage is a requirement. Another success of this method has been the initial tracking of the crushing evolution. One can imagine that as crushing changes the grain size distribution, this method might provide a linkage between stress level and grain and pore size distribution which will be directly linked to permeability.

The statistical method was developed for the cases of strength being either dependent or independent of particle size. Of course the probability distributions used here were rather arbitrary. Potential users of such methods would need to discover and input the distributions relevant to their study in the equations presented here to get crushing predictions. One can imagine the following experimental sequence. A series of single-particle crushing tests is conducted, large enough to obtain an accurate estimate of the probability density of particle strength. Computer simulations of a sample with a similar grain size distribution are then conducted in order to estimate the pdf of particle force. The two functions are combined using the equations presented above to yield the probability of crush of one particle. This might become an alternative or an adjunct to sample element testing.

As mentioned above, this statistical approach becomes inaccurate when crushing events stop being independent. Current work attempts to extend the statistical prediction of crushing by investigating the case when crushing becomes so widespread that events are affecting neighbouring particles. The probability of further crushing events given that a particle has already crushed is therefore our aim. Such methods must hold the key to understanding why localisation might occur.

Acknowledgements

The first author would like to thank the A.S. Onassis Foundation and the A.G. Leventis Foundation for their generous financial support.

References

- Åström, J.A., Herrmann, H.J., 1998. Fragmentation of grains in a two-dimensional packing. *Eur. Phys. J. B* 5, 551–554.
- Baud, P., Klein, E., Wong, T.-F., 2004. Compaction localization in porous sandstones: spatial evolution of damage and acoustic emission activity. *J. Struct. Geol.* 26 (3), 603–624.
- Cheng, Y.P., Bolton, M.D., Nakata, Y., 2004. Crushing and plastic deformation of soils simulated using DEM. *Geotechnique* 54 (2), 131–141.
- Couroyer, C., Ning, Z., Ghadiri, M., 2000. Distinct element analysis of bulk crushing: effect of particle properties and loading rate. *Powder Technol.* 109, 241–254.
- Cundall, P.A., Strack, O.D.L., 1979. A discrete numerical model for granular assemblies. *Geotechnique* 29 (1), 47–65.
- Einav, I., 2007. Breakage mechanics. Part I: theory. *J. Mech. Phys. Solids* 55 (6), 1274–1297.
- Itasca Consulting Group Inc., 2003. PFC^{3D}: Particle Flow Code in 3 Dimensions, Version 3.0, Minneapolis, USA.
- Marketos, G., Bolton, M.D., 2005. Compaction bands as observed in DEM simulations. in: Garcia-Rojo, R., Herrmann, H.J., McNamara, S. (Eds.), *Proceedings of the International Conference of Powders and Grains*, vol. 2. A.A. Balkema, Stuttgart, Germany, pp. 1405–1409.
- McDowell, G.R., Amon, A., 2000. The application of Weibull statistics to the fracture of soil particles. *Soils Found.* 40 (5), 133–141.
- McDowell, G.R., Bolton, M.D., 1998. On the micromechanics of crushable aggregates. *Geotechnique* 48 (5), 667–679.
- Muir Wood, D., 2006. Geomaterials with changing grading: a route towards modelling. in: Hyodo, M., Murata, H., Nakata, Y. (Eds.), *Proceedings of the International Symposium on Geomechanics and Geotechnics of Particulate Media*, Taylor & Francis/Balkema, Ube, Japan, pp. 313–318.
- Nakata, Y., Hyde, A.F.L., Hyodo, M., Murata, H., 1999. A probabilistic approach to sand particle crushing in the triaxial test. *Geotechnique* 49 (5), 567–583.
- Radjai, F., Jean, M., Moreau, J.-J., Roux, S., 1996. Force distributions in dense two-dimensional granular systems. *Phys. Rev. Lett.* 77 (2), 274–277.

- Thornton, C., 1997. Force transmission in granular media. *KONA* 15, 81–90.
- Török, J., Fazekas, S., Unger, T., Wolf, D.E., 2005. Relationship between particle size and normal force. in: Garcia-Rojo, R., Herrmann, H.J., McNamara, S. (Eds.), *Proceedings of the International Conference of Powders and Grains*, vol. 2. A.A. Balkema, Stuttgart, Germany, pp. 1273–1277.
- Tsoungui, O., Vallet, D., Charmet, J.-C., 1999. Numerical model of crushing of grains inside two-dimensional granular materials. *Powder Technol.* 105, 190–198.